

Observation of a Local Structural Change at T_c for $Tl_2Ba_2CaCu_2O_8$ by Pulsed Neutron Diffraction

B. H. Toby and T. Egami

*Department of Materials Science and Engineering and Laboratory for Research on the Structure of Matter,
University of Pennsylvania, Philadelphia, Pennsylvania 19104-6272*

J. D. Jorgensen

Materials Science Division, Argonne National Laboratory, Argonne, Illinois 60439

M. A. Subramanian

*Central Research and Development Department, E. I. du Pont de Nemours and Company,
Experimental Station, Wilmington, Delaware 19898*

(Received 14 March 1990)

Deviations in atomic positions from those of the average crystallographic structure of superconducting $Tl_2Ba_2CaCu_2O_8$ were studied by pair-distribution function (PDF) analysis of pulsed-neutron-scattering data. The PDF shows a clear change in the local structure at the onset of superconductivity. In addition to the previously observed local displacements of Tl and O within the Tl-O sheets, correlated displacements of O and Cu perpendicular to the Cu-O plane have been found. The arrangement of the O atoms appears to be different above and below T_c .

PACS numbers: 61.12.-q, 61.60.+m, 74.70.Vy

The structures of the family of related superconductors $Tl_2Ba_2Ca_{n-1}Cu_nO_{2n+4}$, where $n=1, 2$, and 3 , have been studied extensively by single-crystal and powder-diffraction techniques.¹⁻⁷ In all three materials, evidence for "disorder" in the Tl-O planes has been presented.^{4,5} Previous analysis of pair-distribution functions from powder-diffraction data has demonstrated that the Tl and the coplanar O(3) atom in $Tl_2Ba_2CaCu_2O_8$, a superconductor with T_c of 110 K, are not disordered but have locally correlated displacements that do not exhibit long-range order.⁷ In this work we also demonstrate short-range correlated displacements in the Cu-O(1) plane in this material. These displacements change at the onset of superconductivity. This is the first observation of a structural change correlating with T_c by diffraction.

Atomic pair-distribution functions (PDF's), which describe the distribution of interatomic distances, are commonly used for the study of noncrystalline materials but also have utility for the study of crystalline materials. The PDF is computed from the Fourier transform of the atom-atom interference function $S(Q)$ which incorporates both Bragg and diffuse scattering. Computation of the PDF does not assume local or translational symmetry, in contrast to crystallographic analysis. If a material has local deviations from the average positions, in crystallographic analysis they will be seen as disorder, often expressed as artificially enlarged thermal factors, while in PDF analysis they will be manifest as shifts in the PDF peaks. Thus PDF analysis is able to distinguish between random and correlated deviations, while crystallographic analysis cannot.

For this study, powder-diffraction data were collected using the time-of-flight technique at the special environ-

ment powder diffractometer at the Intense Pulsed Neutron Source of the Argonne National Laboratory.⁸ Approximately 13 g of sample sealed in a vanadium can with He exchange gas was cooled in a Displex He refrigerator. A total of 32 complete data sets were collected at a number of fixed temperatures. To minimize any systematic effects, data were recorded during both stepwise cooling and warming cycles. The PDF, weighted by the neutron cross sections, was obtained by a standard procedure,⁹ with damping of the interference function $S(Q)$ applied from 20 to 30 \AA^{-1} .

The phonon density of states for this material was measured by inelastic neutron diffraction using the IN1 triple-axis neutron diffractometer at the Institut Laue-Langevin. From this result, average thermal vibration amplitudes and the temperature dependence of the PDF peak heights were computed and compared to the actual changes in the heights of individual PDF peaks as a function of temperature. The most striking change with temperature, the height of the 3.4- \AA peak relative to the surrounding minima, is shown in Fig. 1. Since measurements were made under identical conditions, and termination of the Fourier summation was performed at sufficiently high Q values, largely eliminating the termination errors, the most significant source of relative error between points in Fig. 1 is expected from counting statistics. The error estimates for $\rho(r)$ were computed by error propagation. The large change in the PDF at 3.4 \AA in the region just below T_c (110 K) is clearly statistically significant. Rietveld analysis of the diffractograms showed no noticeable changes in any structural parameters with temperature that could account for this change in the PDF, so this structural change can be presumed to have only short-range correlation. Indeed

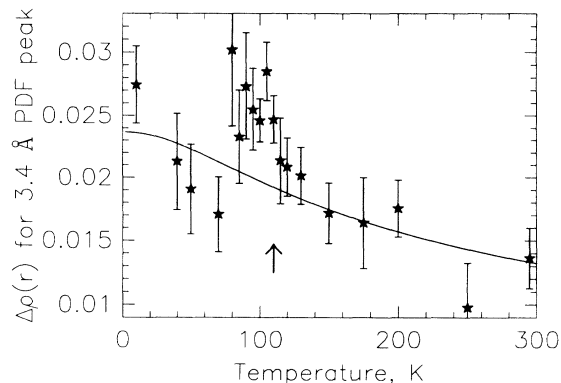


FIG. 1. Change in the PDF for the 3.4-Å peak relative to the average of the surrounding minima. Error bars are drawn at $\pm 1\sigma$, where σ represents the estimated standard deviation from counting statistics. The solid line represents the expected change computed from the phonon density of states. The arrow indicates T_c (110 K).

the differences in the PDF near T_c compared to those above and well below T_c are most significant for r below 6 Å. However, the correlation length cannot be reliably estimated from this measurement.

Modeling was performed by comparison of an observed PDF to a PDF simulated for a trial structure. Simulated PDF's were computed by tabulating interatomic distances for an expanded unit cell with 60 or 240 atoms. This results in a PDF of δ functions which is convoluted with a Gaussian function with the width determined from the phonon density of states, simulating broadening due to thermal motion. An agreement factor A is computed for comparison of observed and simulated PDF results over the range R_{\min} to R_{\max} using

$$A = \frac{1}{\rho_0} \left(\frac{1}{R_{\max} - R_{\min}} \int_{R_{\min}}^{R_{\max}} [\rho_{\text{obs}}(r) - \rho_{\text{calc}}(r)]^2 dr \right)^{1/2},$$

where ρ_0 is the average number density, $\rho_{\text{obs}}(r)$ and $\rho_{\text{calc}}(r)$ are the observed and simulated PDF's, respectively. For this work, the integration range was chosen as 1.5–10 Å.

A Monte Carlo structure refinement process, where changes are made to selected structural parameters using a probabilistic comparison of the agreement between the observed and computed PDF before and after each change, was used to develop structural models. While the previously published model, incorporating correlated displacements of the coplanar Tl and O(3) gives fair agreement to the observed PDF (Fig. 2), the improved statistics of the current data allowed additional structural details to be determined. Introduction of disorder into the copper-oxide layers by allowing multiple sites with partial occupancies for O(1) (the oxygen in the CuO_2 plane), Cu, and/or O(2) (the apically bonded oxygen) gave significant improvement to the agreement between model and observed PDF, as shown in Table I. Even

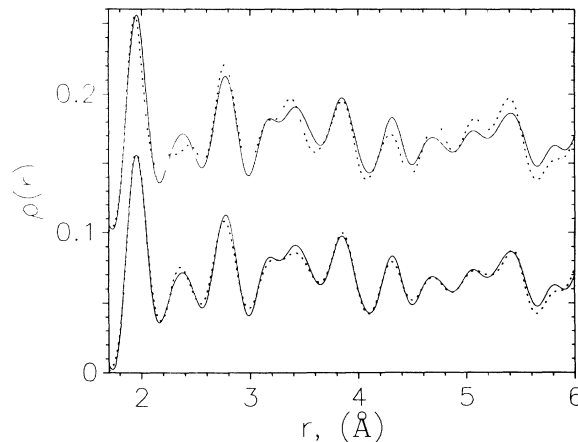


FIG. 2. Atomic pair-distribution functions (PDF's) for $\text{Tl}_2\text{Ba}_2\text{CaCu}_2\text{O}_8$: experimentally determined near 120 K (lower and upper plots, solid line) and modeled, as fitted with only correlated Tl and O(3) displacements (upper plot, dotted line); as fitted with correlated O(1), O(2), and Cu displacements in addition to Tl and O(3) (lower plot, dotted line).

better agreements were obtained with models incorporating both correlated Tl-O(3), Cu-O(1), and O(2) displacements. To improve statistics, modeling was performed on composite PDF patterns for runs between 115 and 130 K, between 95 and 105 K, and between 40 and 70 K; which will be referred to, respectively, as “above T_c ,” “just below T_c ,” and “low T ” in the subsequent discussion.

A large number of models were surveyed and the two which gave the best agreement with the smallest number of parameters are shown in Figs. 3(a) and 3(b), with agreement factors given in Table II. In these models the adjacent CuO_2 sheets are asymmetric, one “buckled” and one “flat.” The buckled sheet has large O(1) displacements and the flat sheet has much smaller O(1) displacements. Approximately half of the Cu atoms are

TABLE I. Agreement factors (as defined in text) for several models compared to the average PDF for five data sets between 115 and 130 K. All models assume $I4/mmm$ symmetry other than correlated Tl-O displacements.

Model description	Agreement
Published coordinates with a fourfold O(3) disorder ^a	0.1800
Refinement of correlated O(3) and Tl displacements ^b	0.0937
Correlated O(3) and Tl displacements plus disordered displacements of Cu, O(1), and O(2)	0.0792

^aReference 5.

^bReference 7.

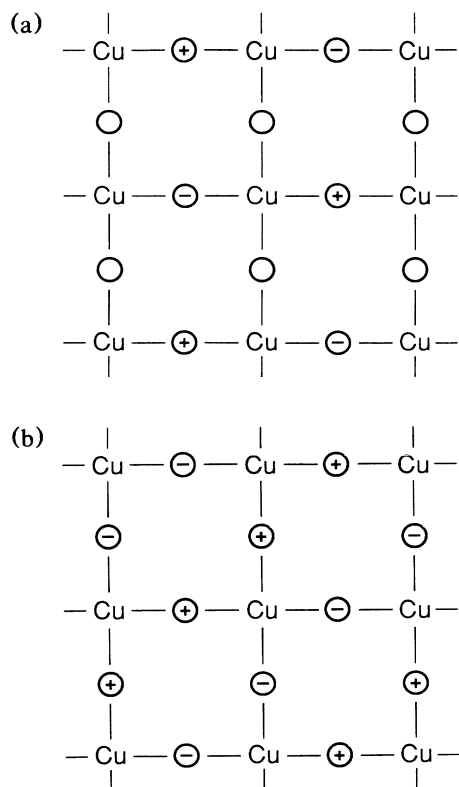


FIG. 3. Schematic representation for O(1) displacements for the correlated displacement models which gave best agreement (a) above T_c and (b) near and below T_c . The + and - signs indicate perpendicular displacement of oxygen toward and away from the Ca sheet, respectively.

displaced in each sheet, with larger Cu displacements in the flat sheet. Similar structures were noted in all models that gave the best agreement, giving us confidence in these results, even though we cannot claim that these models are unique.

Above T_c , the $\langle 100 \rangle$ model shown in Fig. 3(a) gave optimum agreement. In the buckled sheet of this model, one $\langle 100 \rangle$ row of O(1) atoms has alternating 0.35-Å displacements while the other $\langle 100 \rangle$ row of O(1) has fixed displacements of approximately 0.1 Å away from the Ca sheet. In the buckled sheet the Cu atoms are displaced by approximately 0.1 Å toward Ca and in the flat sheet every other Cu atom is displaced by 0.3 Å away from Ca.

The $\langle 110 \rangle$ model shown in Fig. 3(b), with alternating $\langle 110 \rangle$ rows of displaced O(1) atoms and again with one-half of the Cu atoms displaced, gave somewhat better agreement just below T_c and at low T . Just below T_c , the optimum fit yields O(1) displacements of 0.2 Å away from the Ca sheet, and 0.3 Å toward the Ca sheet and Cu displacements of approximately 0.2 Å for the buckled sheet and 0.3 Å for the flat sheet, toward the Ca sheet and away from the Ca sheet, respectively. At low T , the displacements of O(1) were slightly smaller and Cu dis-

TABLE II. Agreement factors for the two models presented in the text for the averaged PDF patterns. Also listed is the statistically estimated minimum expected agreement factor.

Temperature range	$\langle 100 \rangle$ model	$\langle 110 \rangle$ model	Minimum expected
Above T_c (115–130 K)	0.0511	0.0524	0.0127
Just below T_c (95–105 K)	0.0591	0.0539	0.0105
Low T (40–70 K)	0.0589	0.0554	0.0202

placements decreased to approximately 0.15 Å for the buckled sheet and 0.2 Å for the flat sheet.

The differences among the best models for each temperature zone are in excellent qualitative agreement with the actual differences in the experimental PDF's below 4 Å, including the height of the 3.4-Å peak. These differences are not reproduced if the same O displacement pattern is assumed above and below T_c . For this reason, even though the differences in the agreement factor between the $\langle 100 \rangle$ and $\langle 110 \rangle$ models are rather small, we believe that a change in the pattern of O(1) buckling through T_c as suggested by modeling is true. Confirmation of the changes in the short-range order through T_c will require diffuse scattering measurements from a single crystal.

It is interesting to note that the pattern in Fig. 3(a) corresponds to a case of coherently superimposed $[110]$ tilt and $[1\bar{1}0]$ tilt of CuO_4 , considered by Axe *et al.* for $\text{La}_{2-x}\text{Ba}_x\text{CuO}_4$, where subtle local structural changes are shown to have a significant effect on superconductivity.¹⁰ In both the $\langle 100 \rangle$ and $\langle 110 \rangle$ models the average displacement for O(2) remained fairly constant at approximately 0.15 Å, but correlation between the O(2) and the O(1)-Cu displacements is difficult to discern. Even though Tl, O(3), and Ba were allowed to move along the z axis, their displacements are below the expected sensitivity for this technique (0.03 Å). The center-of-mass positions for all atoms in the models are consistent with the crystallographic values. There is reason to believe that the displacement of O atoms is not static but dynamic. We found that the magnitude of the change in the 3.4-Å PDF peak at T_c is larger when the PDF is obtained from the 90° detectors alone than from the 150° detectors. Such a dependence is expected for dynamic displacements, since the pulsed-neutron-scattering data include both elastic- and inelastic-scattering intensities, leading to a dependence of total scattering with incident neutron energy and therefore detector angle.

A possible origin of the oxygen displacement is the repulsion between the holes on O atoms and the Cu ion. The asymmetry of the O displacement of the two CuO_2 sheets may reflect the tendency of holes to segregate through coupling to spin fluctuations of the Cu.¹¹ In particular, the O atoms displaced toward Ca would at-

tract a higher density of holes, making the exchange coupling between the neighboring Cu spins ferromagnetic. In fact, the $\langle 100 \rangle$ model in Fig. 3(a) can be seen as a dimerized Cu pattern due to oxygen atoms with a minus sign. This pattern will tend to localize the holes so that conduction will occur by hopping. The pattern drastically changes at T_c , leading to delocalized holes. The $\langle 110 \rangle$ pattern is identical to the buckling of the CuO_2 sheet in orthorhombic La_2CuO_4 , except that the pattern here is believed to be dynamic and short range. This may reflect the dynamic charge-density wave suggested early in the study of $\text{La}_{2-x}(\text{Sr,Ba})_x\text{CuO}_4$.¹²

The change in the pattern of O displacements at T_c may explain the softening of the phonon mode in $\text{YBa}_2\text{Cu}_3\text{O}_7$ observed by Raman scattering,¹³ and may be related to the dynamical change suggested by ion channeling¹⁴ and the change in the position of the axial oxygen suggested by extended x-ray-absorption fine structure,¹⁵ though the details of the link are unclear. The complexity of the structure revealed by the present work suggests that any theory which is based upon the average crystallographic structure without local distortions may be unrealistic. It also suggests that the mechanism of superconductivity involves strong electron-lattice interactions, enhanced possibly by an inhomogeneous carrier distribution.

The authors are grateful to E. Mele for suggesting the pattern shown in Fig. 3(a), to P. K. Davies and V. Emery for useful discussions, and to W. Dmowski and H. D. Rosenfeld for assistance with data collection and analysis. Work at the University of Pennsylvania was supported by the National Science Foundation through Grants No. DMR-8617950 and No. DMR-8819885. The Intense Pulsed Neutron Source is operated as a user facility by the U.S. Department of Energy, Division of Materials Sciences, under Contract No. W-31-109-Eng-38.

¹S. S. P. Parkin, V. Y. Lee, E. M. Engler, A. I. Nazzari, T. C. Huang, G. Gorman, R. Savoy, and R. Beyers, *Phys. Rev. Lett.* **60**, 2539 (1988).

²R. Beyers, S. S. P. Parkin, V. Y. Lee, A. I. Nazzari, R. Savoy, G. Gorman, T. C. Huang, and S. LaPlaca, *Appl. Phys. Lett.* **53**, 432 (1988).

³R. M. Hazen, L. W. Finger, R. J. Angel, C. T. Prewitt, N. L. Ross, C. G. Hadjidakos, P. J. Heaney, D. R. Velten, Z. Z. Sheng, A. El Ali, and A. M. Hermann, *Phys. Rev. Lett.* **60**, 1657 (1988).

⁴M. A. Subramanian, J. C. Calabrese, C. C. Torardi, J. Gopalakrishnan, T. R. Askew, R. B. Flippen, K. J. Morrissey, U. Chowdhry, and A. W. Sleight, *Nature (London)* **332**, 420 (1988).

⁵D. E. Cox, C. C. Torardi, M. A. Subramanian, J. Gopalakrishnan, and A. W. Sleight, *Phys. Rev. B* **38**, 6624 (1988).

⁶A. W. Hewat, E. A. Hewat, J. Brynstad, H. A. Mook, and E. D. Specht, *Physica (Amsterdam)* **152C**, 438 (1988).

⁷W. Dmowski, B. H. Toby, T. Egami, M. A. Subramanian, J. Gopalakrishnan, and A. W. Sleight, *Phys. Rev. Lett.* **61**, 2608 (1988).

⁸J. D. Jorgensen, J. Faber, J. M. Carpenter, R. K. Crawford, J. R. Haumann, R. L. Hitterman, R. Lueb, G. E. Ostrowski, R. J. Rotella, and T. G. Worlton, *J. Appl. Cryst.* **22**, 321 (1989).

⁹S. Nanao, W. Dmowski, T. Egami, J. W. Richardson, Jr., and J. D. Jorgensen, *Phys. Rev. B* **35**, 435 (1987).

¹⁰J. D. Axe, A. H. Moudden, H. Hohlwein, D. E. Cox, K. M. Mohanty, A. R. Moodenbaugh, and Y. Xy, *Phys. Rev. Lett.* **62**, 2751 (1989).

¹¹V. J. Emery, S. A. Kivelson, and H. Q. Lin, *Phys. Rev. Lett.* **64**, 475 (1990).

¹²J. D. Jorgensen, H. B. Schuttler, D. G. Hinks, D. W. Capone, II, K. Zhang, M. B. Brodsky, and D. J. Scalapino, *Phys. Rev. Lett.* **58**, 1024 (1987).

¹³C. Thomsen, M. Cardona, B. Gegenheimer, R. Liu, and A. Simon, *Phys. Rev. B* **37**, 9860 (1988).

¹⁴R. P. Sharma, L. E. Rehn, P. M. Baldo, and J. Z. Liu, *Phys. Rev. Lett.* **62**, 2869 (1989).

¹⁵S. D. Conradson and I. D. Raistrick, *Science* **243**, 1340 (1989).